Author(s): Armstrong, Andrea; Chivers, Tristram; Tuononen, Heikki; Parvez, Masood

Title: Synthesis and Structures of Aluminum and Magnesium Complexes of Tetraimidophosphates and Trisamidothiophosphates: EPR and DFT Investigations of the Persistent Neutral Radicals {Me2Al[(μ-NR)(μ-NtBu)P(μ-NtBu)2]Li(THF)2}• (R = SiMe3, tBu)

Year: 2005

Version:

Please cite the original version:

Armstrong, A., Chivers, T., Tuononen, H., & Parvez, M. (2005). Synthesis and Structures of Aluminum and Magnesium Complexes of Tetraimidophosphates and Trisamidothiophosphates: EPR and DFT Investigations of the Persistent Neutral Radicals {Me2Al[(μ-NR)(μ-NtBu)P(μ-NtBu)2]Li(THF)2}• (R = SiMe3, tBu). Inorganic Chemistry, 44(16), 5778-5788. https://doi.org/10.1021/ic050689e

Synthesis and Structures of Aluminum and Magnesium Complexes of Tetraimidophosphates and Trisamidothiophosphates: EPR and DFT Investigations of the Persistent Neutral Radicals $\{Me_2Al[(\mu\text{-}NR)(\mu\text{-}N^tBu)P(\mu\text{-}N^tBu)_2]Li(THF)_2\}^{\bullet}$ (R = $SiMe_3$, ^tBu)

Andrea Armstrong, Tristram Chivers,* Heikki M. Tuononen, and Masood Parvez

Department of Chemistry, University of Calgary, Calgary, Alberta, Canada T2N 1N4

* To whom correspondence should be addressed.
Telephone: (403) 220-5741
Fax: (403) 289-9488
E-mail: chivers@ucalgary.ca

Abstract

Reactions of $(RNH)_3PNSiMe_3$ (**3a**, R = ^{t}Bu; **3b**, R = Cy) with trimethylaluminum result in the formation of $\{Me_2Al(\mu\text{-}N^tBu)(\mu\text{-}NSiMe_3)P(NH^tBu)_2]\}$ (**4**) and the dimeric trisimidometaphosphate $\{Me_2Al[(\mu\text{-}NCy)(\mu\text{-}NSiMe_3)P(\mu\text{-}NCy)_2P(\mu\text{-}NCy)(\mu\text{-}NSiMe_3)]AlMe_2\}$ (**5a**), respectively. The reaction of $SP(NH^tBu)_3$ (**2a**) with one or two equivalent of $AlMe_3$ yields $\{Me_2Al[(\mu\text{-}S)(\mu\text{-}N^tBu)P(NH^tBu)_2]\}$ (**7**) and $\{Me_2Al[(\mu\text{-}S)(\mu\text{-}N^tBu)P(\mu\text{-}NH^tBu)(\mu\text{-}N^tBu)]AlMe_2\}$ (**8**), respectively. Metallation of **4** with ^{n}BuLi produces the heterobimetallic species $\{Me_2Al[(\mu\text{-}N^tBu)(\mu\text{-}NSiMe_3)P(\mu\text{-}NH^tBu)(\mu\text{-}N^tBu)]Li(THF)_2\}$ (**9a**) and $\{[Me_2Al][Li]_2[P(N^tBu)_3(NSiMe_3)]\}$ (**10**) sequentially; in THF solutions, solvation of **10** yields an ion pair containing a spirocyclic tetraimidophosphate monoanion. Similarly, the reaction of $(^tBuNH)_3PN^tBu$ with $AlMe_3$ followed by two equivalents of ^{n}BuLi generates $\{Me_2Al[(\mu\text{-}N^tBu)_2P(\mu_2\text{-}N^tBu)_2(\mu_2\text{-}THF)[Li(THF)]_2\}$ (**11a**). Stoichiometric oxidations of **10** and **11a** with iodine yield the neutral spirocyclic radicals $\{Me_2Al[(\mu\text{-}NR)(\mu\text{-}N^tBu)P(\mu\text{-}N^tBu)_2]Li(THF)_2\}^{\bullet}$ (**13a**, R = $SiMe_3$; **14a**, R = ^{t}Bu) which have been characterized by EPR spectroscopy. DFT calculations confirm the retention of the spirocyclic structure and indicate that the spin density in these radicals is concentrated on the nitrogen atoms of the PN_2Li ring. When **3a** or **3b** is treated with half-an-equivalent of dibutylmagnesium, the complexes $\{Mg[(\mu\text{-}N^tBu)(\mu\text{-}NH^tBu)P(NH^tBu)(NSiMe_3)]_2\}$ (**15**) and $\{Mg[(\mu\text{-}NCy)(\mu\text{-}NSiMe_3)P(NHCy)_2]_2\}$ (**16**) are obtained, respectively. Addition of half-an-equivalent of $MgBu_2$ to **2a** results in the formation of $\{Mg[(\mu\text{-}S)(\mu\text{-}N^tBu)P(NH^tBu)_2]_2\}$ (**17**), which produces the hexameric species $\{[MgOH][(\mu\text{-}S)(\mu\text{-}N^tBu)P(NH^tBu)_2]\}_6$ (**18**) upon hydrolysis. Compounds **4**, **5a**,

7-11a, and **15-17** have been characterized by multinuclear (^{1}H, ^{13}C, and ^{31}P) NMR spectroscopy and, in the case of **5a**, **9a**•2THF, **11a**, and **18,** by X-ray crystallography.

Introduction

One of the more active areas of main group chemistry research over the past decade has been the synthesis and characterization of imido analogues of simple oxoanions such as carbonate, silicate and phosphate.[1] The underlying principle of this work is that the oxo units $[O]^{2-}$ of these species are formally isoelectronic[2] with the imido $[NR]^{2-}$ (R= H, alkyl, aryl) group, and thus a new class of p-block polyanions can be generated by substituting some, or all, of the oxygen atoms by imido groups. The chemical and physical properties of these polyimido anions are dependent in large part upon the ratio of imido:oxo units and the size of the imido substituent.[1]

Numerous analogues of phosphorus oxo-anions have been prepared,[3] including the trisimido(meta)phosphate[4] $[P(NR)_3]^-$ and tetraimido(ortho)phosphate $[P(NR)_3(NR')]^{3-}$ (R = R′ = naphthyl;[5] R = ^{t}Bu, R′ = $SiMe_3$[6]) trianions. Heteroleptic systems, such as the trisimido-phosphate and -thiophosphate trianions $[EP(NR)_3]^{3-}$ (E = O,[7] S[8]), have also been reported recently and the first transition-metal derivatives of the sulfur-containing ligand have been characterized.[9]

Previously we have thoroughly investigated the reactivities of a series of trisaminophosphates $OP(NH^tBu)_3$ (**1**),[6, 8] $SP(NHR)_3$ (**2a**, R = ^{t}Bu; **2b**, R = ^{i}Pr; **2c**, R = *p*-tol)[8, 10] and $(RNH)_3PNSiMe_3$ (**3a**, R = ^{t}Bu; **3b**, R = Cy)[6, 11] toward alkyllithium reagents. It was found that the reactivity of these aminophosphate species increases across the series **1** < **2** < **3**. Specifically, threefold deprotonation of **1, 2a** or **2b** is not possible using

n-butyllithium, whereas it does occur for **2c** and is readily effected for both **3a** and **3b**. More recently, we have prepared a series of zinc imidophosphates by the reactions of **1**, **2a, 3a** and **3b** with dimethylzinc.[7] Interestingly, the reaction of **1** with $ZnMe_2$ generated several products via at least two distinct reaction pathways, whereas the reaction of **3a** and dimethylzinc produced only $\{MeZn[(\mu\text{-}N^tBu)(\mu\text{-}NSiMe_3)P(NH^tBu)_2]\}$. In addition, two zinc complexes were isolated that contained the trisimidophosphate trianion $[OP(N^tBu)_3]^{3-}$, which had not been observed in earlier reactions between **1** and *n*-butyllithium, trimethylaluminum, or lithium aluminum hydride.[12]

The only known main group metal complexes of **2** and **3** are their lithium derivatives. In view of the current interest in aluminophosphates,[13] the development of synthetic routes to a family of polyimido-aluminophosphates is certainly a worthwhile endeavor. To this end, we have examined the reactions of **2a** and **3** with trimethylaluminum. While it is not possible to effect the three-fold deprotonation of **1** with trimethylaluminum,[12] the possibility of preparing trisimido(thio)- or tetraimido aluminophosphates remains. Reactions of **1**-**3** with $MgBu_2$ have also been investigated in order to gain a better understanding of the reactivity of these amido reagents towards metal alkyls.

Experimental

Reagents and General Procedures. All experiments were carried out under an argon atmosphere using standard Schlenk techniques. Toluene, *n*-hexane, diethyl ether and tetrahydrofuran (THF) were dried over Na/benzophenone, distilled, and stored over molecular sieves prior to use. Trimethylaluminum (2.0 M solution in toluene), ^{n}BuLi

(2.5 M solution in hexanes), and $MgBu_2$ (1.0 solution in heptane) were used as received from Aldrich. Iodine was sublimed prior to use. $(RNH)_3PNSiMe_3$ (R = ^{t}Bu, Cy),[6] $SP(NH^tBu)_3$[8] and $OP(NH^tBu)_3$[8] were prepared as described previously.

Instrumentation. ^{1}H, ^{7}Li, ^{13}C and ^{31}P NMR spectra were collected on a Bruker DRX-400 spectrometer with chemical shifts reported relative to Me_4Si in $CDCl_3$ (^{1}H and ^{13}C), LiCl in D_2O (^{7}Li) and 85 % H_3PO_4 in D_2O (^{31}P). All spectra were collected at 22 ºC. Infrared spectra were recorded as Nujol mulls on KBr plates using a Nicolet Nexus 470 FTIR spectrometer in the range 4000 - 400 cm^{-1}. EPR spectra were recorded at 22 ºC on a Bruker EMX 113 spectrometer; spectral simulations were carried out using XEMR[14] and WINEPR SimFonia.[15] Elemental analyses were provided by the Analytical Services Laboratory, Department of Chemistry, University of Calgary.

Preparation of $\{Me_2Al[(\mu\text{-}N^tBu)(\mu\text{-}NSiMe_3)P(NH^tBu)_2]\}$ (4).

A solution of $AlMe_3$ (0.60 mL, 2.0 M, 1.2 mmol) in toluene was added to a clear, colorless solution of $(^tBuNH)_3PNSiMe_3$ (0.404 g, 1.21 mmol) in hexane (20 mL) at 22 ^{o}C. After 3 h, the solvent was removed in vacuo, and the product was washed with hexane (5 mL) leaving **4** as an off-white powder (0.339 g, 0.868 mmol, 72 %). ^{1}H NMR (C_6D_6, δ): 1.8 (br, 2 H, N*H*), 1.29 [d, 9 H, N^{t}Bu], 1.16 [d, 18 H, NH^t*Bu*], 0.34 (s, 9 H, $SiMe_3$), -0.22 (s, 6 H, $AlMe_2$). ^{13}C NMR (C_6D_6, δ): 51.76 [d, N*C*Me_3, ^2J(^{13}C-^{31}P) = 10.9 Hz], 50.63 [d, NH*C*Me_3, ^2J(^{13}C-^{31}P) = 15.2 Hz], 33.01 [d, NC*Me*$_3$, ^3J(^{13}C-^{31}P) = 34.2 Hz], 32.30 [d, NHC*Me*$_3$, ^3J(^{13}C-^{31}P) = 15.5 Hz], 3.57 [d, $SiMe_3$, ^3J(^{13}C-^{31}P) = 14.9 Hz], 1.37 (s, $AlMe_2$). ^{31}P{^{1}H} NMR (C_6D_6, δ): 5.6 (s). IR (Nujol): 3404 cm^{-1} (ν N-H). Anal.

Calcd. for $C_{17}H_{44}N_4AlPSi$: C, 52.27; H, 11.35; N, 14.34. Found: C, 52.16; H, 12.03; N, 13.92.

Preparation of {$Me_2Al[(\mu\text{-}NCy)(\mu\text{-}NSiMe_3)P(\mu\text{-}NCy)_2P(\mu\text{-}NCy)(\mu\text{-}NSiMe_3)]AlMe_2$} (5a).

A solution of $AlMe_3$ (0.35 mL, 2.0 M, 0.70 mmol) in toluene was added to a clear, colorless solution of $(CyNH)_3PNSiMe_3$ (0.286 g, 0.693 mmol) in hexane (20 mL) at 22 ºC. The reaction mixture was stirred for 15 h; the volume of the solution was then reduced to 1 mL and stored at -18 ºC. After 48 h, colorless crystals of **5a** were obtained (0.226 g, 0.306 mmol, 88.3 %). ^{1}H NMR (C_6D_6, δ): 0.8-1.9 (m, Cy), 0.22 (s, 18 H, $SiMe_3$), -0.37 (s, 6 H, $AlMe_2$). ^{13}C NMR (C_6D_6, δ): 51.68 (s, *C*Me_3), 50.05 (s, *C*Me_3), 37.78 [d, NC*C*H_2, $^3J(^{13}C\text{-}^{31}P)$ = 35.6 Hz], 36.91 [d, NC*C*H_2, $^3J(^{13}C\text{-}^{31}P)$ = 19.2 Hz], 36.78 [d, NC*C*H_2, $^3J(^{13}C\text{-}^{31}P)$ = 18.4 Hz], 26.18 (s, NCCH$_2$*C*H_2), 25.94 (s, NCCH$_2$*C*H_2), 25.78 (s, *p*-CH_2), 2.67 [d, $SiMe_3$, $^3J(^{13}C\text{-}^{31}P)$ = 14.0 Hz], -6.81 (s, $AlMe_2$). $^{31}P\{^1H\}$ NMR (C_6D_6, δ): 17.1 (s). CHN analyses gave high C values owing to difficulties with the complete removal of $CyNH_2$.

Preparation of {$Me_2Al[(\mu\text{-}S)(\mu\text{-}N^tBu)P(NH^tBu)_2]$} (7).

A solution of $AlMe_3$ (2.25 mL, 2.0 M, 4.5 mmol) in toluene was added to a clear, colorless solution of $SP(NH^tBu)_3$ (1.24 g, 4.44 mmol) in toluene (25 mL) at 22 ºC. After 24 h, the solvent was removed in vacuo, leaving a colorless oil; after storage for 12 h, the product had solidified giving **7** as a white powder (1.25 g, 3.73 mmol, 82.8 %). ^{1}H NMR (C_6D_6, δ): 1.23 (s, 9 H, N^{t}Bu), 1.18 (s, 18 H, NH^{t}Bu), -0.24 [d, $^4J(^1H\text{-}^{31}P)$ = 1.8 Hz, 6 H,

Me_2Al]. $^{13}C\{^1H\}$ NMR (C_6D_6, δ): 54.32 [d, *C*Me_3, $^2J(^{13}C\text{-}^{31}P)$ = 37.2 Hz], 52.44 [d, *C*Me_3, $^2J(^{13}C\text{-}^{31}P)$ = 9.0 Hz], 33.03 [d, C*Me*$_3$, $^3J(^{13}C\text{-}^{31}P)$ = 34.7 Hz], 31.42 [d, C*Me*$_3$, $^3J(^{13}C\text{-}^{31}P)$ = 18.6 Hz], -5.20 (br, Me_2Al). $^{31}P\{^1H\}$ NMR (C_6D_6, δ): 35.6 (s). Anal. Calcd. for $C_{14}H_{35}N_3PSAl$: C, 50.12; H, 10.52; N, 12.53. Found: C, 49.64; H, 10.97; N, 12.63.

Preparation of {Me_2Al[(μ-S)(μ-N^{t}Bu)P(μ-NH^{t}Bu)(μ-N^{t}Bu)]$AlMe_2$} (8).

A solution of $AlMe_3$ (4.8 mL, 2.0 M, 9.6 mmol) in toluene was added to a clear, colorless solution of $SP(NH^tBu)_3$ (1.30 g, 4.65 mmol) in toluene (20 mL) at 22 ºC. After 40 h, the solvent was removed in vacuo, leaving **8** as a white powder (1.74 g, 4.44 mmol, 95.5 %). ^1H NMR (C_6D_6, δ): 3.30 (br, d, N*H*), 1.33 [d, $^4J(^1H\text{-}^{31}P)$ = 0.9 Hz, 9 H, N^t*Bu*], 1.23 [d, $^4J(^1H\text{-}^{31}P)$ = 0.7 Hz, 9 H, N^t*Bu*], 1.20 [d, $^4J(^1H\text{-}^{31}P)$ = 0.9 Hz, 9 H, NH^t*Bu*], -0.25 (s, 3H, Me_2Al), -0.31 (s, 3 H, Me_2Al), -0.39 (s, 3H, Me_2Al), -0.54 (s, 3 H, Me_2Al). $^{13}C\{^1H\}$ NMR (C_6D_6, δ): 59.09 [d, *C*Me_3, $^2J(^{13}C\text{-}^{31}P)$ = 12.9 Hz], 54.99 [d, *C*Me_3, $^2J(^{13}C\text{-}^{31}P)$ = 39.3 Hz], 53.53 [d, *C*Me_3, $^2J(^{13}C\text{-}^{31}P)$ = 8.8 Hz], 33.23 [d, C*Me*$_3$, $^3J(^{13}C\text{-}^{31}P)$ = 34.0 Hz], 32.33 [d, C*Me*$_3$, $^3J(^{13}C\text{-}^{31}P)$ = 31.2 Hz], 30.05 [d, C*Me*$_3$, $^3J(^{13}C\text{-}^{31}P)$ = 17.9 Hz], -5.20 (br, Me_2Al), -6.09 (br, Me_2Al). $^{31}P\{^1H\}$ NMR (C_6D_6, δ): 40.9 (s). Anal. Calcd. for $C_{16}H_{40}N_3PSAl_2$: C, 49.08; H, 10.30; N, 10.73. Found: C, 49.05; H, 10.72; N, 10.97.

Preparation of {[Me_2Al][Li][P(N^{t}Bu)$_2$(NH^{t}Bu)(NSiMe_3)]} (9a).

A solution of $AlMe_3$ (0.75 mL, 2.0 M, 1.50 mmol) in toluene was added to a stirred solution of (^{t}BuNH)$_3$P$NSiMe_3$ (0.502 g, 1.50 mmol) in hexane (20 mL) at 22 ºC. After 1.5 h, ^{n}BuLi (0.60 mL, 1.50 mmol) was added, resulting in a white slurry. After an

additional 3 h, the solvent was removed in vacuo, leaving **9a** as a white powder (0.582 g, 1.47 mmol, 98 %). Colorless X-ray quality crystals of {$Me_2Al[(\mu\text{-}N^tBu)(\mu\text{-}NSiMe_3)P(\mu\text{-}NH^tBu)(\mu\text{-}N^tBu)]Li(THF)_2$} **9a•**2THF were obtained from a THF/hexane mixture at -18 ºC. ^{1}H NMR (d_8-THF, δ): 1.35 (s, 9 H, ^{t}Bu), 1.31 (s, 9 H, ^{t}Bu), 1.29 (s, 9 H, ^{t}Bu), 0.13 (s, 9 H, $SiMe_3$), -0.89 (d, 6 H, Me_2Al). $^{13}C\{^1H\}$ NMR (d_8-THF, δ): 52.39 (s, *C*Me_3), 51.14 [d, *C*Me_3, $^2J(^{13}C\text{-}^{31}P)$ = 36.3 Hz], 36.70 [d, C*Me*$_3$, $^3J(^{13}C\text{-}^{31}P)$ = 38.7 Hz]), 36.09 [d, C*Me*$_3$, $^3J(^{13}C\text{-}^{31}P)$ = 41.1 Hz], 34.11 [d, C*Me*$_3$, $^3J(^{13}C\text{-}^{31}P)$ = 29.1 Hz]), 33.50 [d, C*Me*$_3$, $^3J(^{13}C\text{-}^{31}P)$ = 19.2 Hz], 14.59 (s, $SiMe_3$), 4.26 (s, $AlMe_2$). $^{31}P\{^1H\}$ NMR (d_8-THF, δ): 8.2 (s). Anal. Calcd. for $C_{17}H_{43}N_4LiAlSiP$: C, 51.49; H, 10.93; N, 14.13. Found: C, 50.90; H, 10.73; N, 14.31.

Preparation of {[Me_2Al][Li]$_2$[$P(N^tBu)_3(NSiMe_3)$]} (10).

A solution of $AlMe_3$ (0.60 mL, 2.0 M, 1.2 mmol) in toluene was added to a stirred pale yellow solution of (^{t}BuNH)$_3$P$NSiMe_3$ (0.404 g, 1.21 mmol) in hexane, resulting in a cloudy off-white solution. After 3h, ^{n}BuLi (0.90 mL, 2.5 M, 2.3 mmol) in hexanes was added to the reaction mixture, resulting in a white slurry. After an additional 3 h, the solvent was removed in vacuo, leaving **10** as a white powder (0.427 g, 1.06 mmol, 93 %). ^{1}H NMR (d_8-THF, δ): 1.32 (s, 9 H, N^{t}Bu), 1.30 (s, 18 H, N^{t}Bu), 0.08 (s, 9 H, $SiMe_3$), -0.94 (s, 6 H, $AlMe_2$). ^{7}Li (d_8-THF, δ): 0.70 (s). ^{7}Li (C_6D_6, δ): 1.44 (s), -2.71(s). $^{13}C\{^1H\}$ NMR (C_6D_6, δ): 50.72 [d, N*C*Me_3, $^2J(^{13}C\text{-}^{31}P)$ = 6.8 Hz], 36.58 [d, NC*Me*$_3$, $^3J(^{13}C\text{-}^{31}P)$ = 36.2 Hz], 33.77 [d, NHC*Me*$_3$, $^3J(^{13}C\text{-}^{31}P)$ = 27.2 Hz], 4.19 (s, $SiMe_3$), -4.61 (s, $AlMe_2$). $^{31}P\{^1H\}$ NMR (d_8-THF, δ): 10.0 (s). Satisfactory CHN analyses could not be obtained due to the extremely hygroscopic nature of this compound.

Preparation of {$Me_2Al[(\mu\text{-}N^tBu)_2P(\mu_2\text{-}N^tBu)_2(\mu_2\text{-}THF)[Li(THF)]_2$} (11a).

A solution of $AlMe_3$ (0.55 mL, 2.0 M, 1.10 mmol) in toluene was added to a stirred clear, colorless solution of $(^tBuNH)_3PN^tBu$ (0.353 g, 1.11 mmol) in hexane (15 mL), resulting in an opaque white solution. After 3 h, ^nBuLi (1.4 mL, 1.6 M, 2.24 mmol) in hexanes was added to the reaction mixture, resulting in a white slurry. After an additional 2.5 h, the white solid was allowed to settle, and the supernatant liquid was decanted. The product was washed with an additional 5 mL of hexane prior to the removal of the solvent in vacuo. The product $\{[Me_2Al][Li]_2[P(N^tBu)_4]\}$ was isolated as a white powder (0.339 g, 0.887 mmol, 80 %). Recrystallization from THF/hexane produced colorless X-ray quality crystals of $\{Me_2Al[(\mu\text{-}N^tBu)_2P(\mu_2\text{-}N^tBu)_2(\mu_2\text{-}THF)[Li(THF)]_2\}$ **11a**. ^1H NMR (d_8-THF, δ): 1.34 (s, 36 H, N^tBu), -0.96 (s, 6 H, $AlMe_2$). ^7Li (d_8-THF, δ): 1.23 (s). $^{13}C\{^1H\}$ NMR (C_6D_6, δ): 50.90 (s, N*C*Me_3), 50.78 [d, N*C*Me_3, $^2J(^{13}C\text{-}^{31}P)$ = 8.3 Hz], 36.41 [d, NC*Me*$_3$, $^3J(^{13}C\text{-}^{31}P)$ = 34.9 Hz], 34.45 [d, NHC*Me*$_3$, $^3J(^{13}C\text{-}^{31}P)$ = 25.4 Hz], -4.0 (br, s, $AlMe_2$). $^{31}P\{^1H\}$ NMR (d_8-THF, δ): 12.4 (s). Satisfactory CHN analyses could not be obtained due to the extremely hygroscopic nature of this compound.

Preparation of {$Mg[(\mu\text{-}N^tBu)(\mu\text{-}NH^tBu)P(NH^tBu)(NSiMe_3)]_2$} (15)

A solution of $MgBu_2$ (1.56 mL, 1.0 M, 1.56 mmol) in heptane was added to a stirred solution of $(^tBuNH)_3PNSiMe_3$ (1.05 g, 3.14 mmol) in hexane (15 mL) at 22 ºC. After 18 h, the solvent was removed in vacuo, leaving **15** as a white solid (0.986 g, 1.42 mmol, 91 %). ^1H NMR (C_6D_6, δ): 1.9 (br, d, NH), 1.8 (br, d, NH), 1.49 (s, 9 H, N^tBu), 1.39 (s, 9 H, NH^tBu), 1.32 (s, 9 H, NH^tBu), 0.50 (s, 9 H, $SiMe_3$). $^{13}C\{^1H\}$ NMR (d_8-

THF, δ): 51.52 (s, *C*Me$_3$), 51.46 (s, *C*Me$_3$), 51.40 (s, *C*Me$_3$), 50.89 [d, *C*Me$_3$, ^2J(^{13}C-^{31}P) = 3.0 Hz], 50.63 [d, *C*Me$_3$, ^2J(^{13}C-^{31}P) = 15.0 Hz], 35.2 (s, C*Me*$_3$), 33.4 [d, C*Me*$_3$, ^3J(^{13}C-^{31}P) = 30.0 Hz], 33.2 [d, C*Me*$_3$, ^3J(^{13}C-^{31}P) = 30.0 Hz], 32.3 [d, C*Me*$_3$, ^3J(^{13}C-^{31}P) = 30.0 Hz], 5.7 [d, SiMe$_3$, ^3J(^{13}C-^{31}P) = 30.0 Hz], 4.3 [d, SiMe$_3$, ^3J(^{13}C-^{31}P) = 30.0 Hz]. ^{31}P{^{1}H} NMR(C_6D_6, δ): 5.2 (s). Anal. Calcd. for $C_{30}H_{76}N_8MgP_2Si_2$: C, 52.11; H, 11.08; N, 16.21. Found: C, 52.20; H, 10.19; N, 15.51.

Preparation of {Mg[(μ-NCy)(μ-NSiMe$_3$)P(NHCy)$_2$]$_2$} (16).

A solution of $MgBu_2$ (0.82 mL, 0.82 mmol) in heptane was added to a stirred solution of $(CyNH)_3PNSiMe_3$ (0.677 g, 1.64 mmol) in hexane (20 mL) at 22 ºC. After 20 h, the solvent was removed in vacuo, leaving **16** as an off-white solid (0.540 g, 0.637 mmol, 78 %). ^{1}H NMR (C_6D_6, δ): 1.0 – 3.2 (br, m, Cy) 0.40 (s, 9 H, $SiMe_3$). ^{13}C{^{1}H} NMR (d_8-THF, δ): 52.71 (s, *C*N), 50.03 [d, *C*NH, ^2J(^{13}C-^{31}P) = 30.4 Hz], 40.26 (s, *C*H$_2$CN), 37.70 [d, *C*H$_2$CNH, ^3J(^{13}C-^{31}P) = 80.0 Hz], 26.73 (s, CH*C*H$_2$), 26.31 (br, s, CH$_2$*C*HCH$_2$), 4.34 (s, Si*Me*$_3$). ^{31}P{^{1}H} NMR (C_6D_6, δ): 19.6 (s). Anal. Calcd. for $C_{42}H_{88}N_8P_2Si_2Mg$: C, 59.51; H, 10.46; N, 13.22. Found: C, 59.46; H, 10.88; N, 12.53.

Preparation of {Mg[(μ-S)(μ-N^{t}Bu)P(NH^{t}Bu)$_2$]$_2$} (17).

A solution of $MgBu_2$ (2.0 mL, 1.0 m, 2.0 mmol) was added to a stirred solution of $SP(NH^tBu)_3$ (1.125 g, 4.026 mmol) in toluene (20 mL) at 22 ºC, resulting in a clear colorless solution. After 20 h, the solvent was removed in vacuo, leaving a colorless oil. After storage for 24 h, **17** was obtained as a white powder (1.077 g, 1.850 mmol, 92.5 %). ^{1}H NMR(C_6D_6, δ): 2.03 (br, d, N*H*), 1.42 (s, 9H, N^t*Bu*), 1.30 (s, 18H, NH^t*Bu*). ^{13}C{^{1}H}

NMR (C_6D_6, δ): 53.32 [d, *C*Me_3, $^2J(^{13}C\text{-}^{31}P)$ = 46.7 Hz], 51.76 [d, *C*Me_3, $^2J(^{13}C\text{-}^{31}P)$ = 8.8 Hz], 34.73 [d, C*Me*$_3$, $^3J(^{13}C\text{-}^{31}P)$ = 41.0 Hz], 31.63 [d, C*Me*$_3$, $^3J(^{13}C\text{-}^{31}P)$ = 16.9 Hz]. $^{31}P\{^1H\}$ NMR (C_6D_6, δ): 38.8 (s). Anal. Calcd. for $C_{24}H_{58}N_6P_2S_2Mg$: C, 49.60; H, 10.06; N, 14.46. Found: C, 50.89; H, 10.62; N, 13.69.

Storage of a solution of **17** in diethyl ether at -18 °C for one week yielded colorless crystals of $\{[MgOH][(\mu\text{-}S)(\mu\text{-}N^tBu)P(NH^tBu)_2]\}_6$ (**18**).

X-ray Analyses. Colorless crystals of **5a**, **9a•**2THF**, 11a** and **18** were coated with Paratone 8277 oil and mounted on a glass fiber. All measurements were made on a Nonius Kappa CCD diffractometer using graphite-monochromated molybdenum-K_α radiation. Crystallographic data are summarized in Table 1. The structures were solved by direct methods[16] and refined by full-matrix least-squares methods using SHELXL-97.[17] Hydrogen atoms were included at geometrically idealized positions and were not refined; the non-hydrogen atoms were refined anisotropically. A cyclohexyl ring in **5a** was disordered in one of the molecules; this was included in the refinements using partial site occupancy factors. Only some of the non-hydrogen atoms in **9a•**2THF were refined anisotropically. The α-carbon of the N^tBu group and the silicon atom $NSiMe_3$ group chelated to the Al atom showed positional disorder with the two atoms occupying the same sites; the model was refined with the C and Si atoms assigned partial occupancies that summed to unity. Carbon atoms of both THF ligands were disordered over two sites with equal site occupancy factors. The hydrogen atom attached to N(4) was located from a difference map.

Computational Details The structures of the model radicals {$Me_2Al[(\mu\text{-}NMe)(\mu\text{-}NSiH_3)P(\mu\text{-}NMe)_2]Li(OMe_2)_2\}^{\bullet}$ (**13b**) and {$Me_2Al[(\mu\text{-}NMe)_2P(\mu\text{-}NMe)_2]Li(OMe_2)_2\}^{\bullet}$ (**14b**) were optimized in their doublet ground states using Density Functional Theory (DFT) and C_s and C_{2v} symmetry, respectively. Hybrid PBE0 exchange-correlation functional[18, 19] and Ahlrichs' triple-zeta valence basis set augmented by one set of polarization functions (TZVP)[20] were used in the optimizations. Hyperfine coupling constants (HFCCs) were then calculated by single-point calculations employing the optimized geometries, PBE0 functional and unrestricted Kohn-Sham formalism. For P, N, Li and Al, the single-point calculations utilized the IGLO-III basis set[21] in a completely uncontracted form and augmented with one additional steep s-function as well as f-polarization functions from the cc-pVTZ basis set.[21] For Si, C and H the calculations utilized the cc-pVTZ basis set[21] in its standard form. A pruned (99,590) integration grid was used in all single point calculations to ensure numerical convergence of calculated HFCCs. All geometry optimizations were done with the Turbomole 5.7[22] program package; Gaussian 03[23] was used in all single point calculations.

Results and Discussion

Synthesis and Characterization of {$Me_2Al[(\mu\text{-}N^tBu)(\mu\text{-}NSiMe_3)P(NH^tBu)_2]$} (4) and {$Me_2Al[(\mu\text{-}NCy)(\mu\text{-}NSiMe_3)P(\mu\text{-}NCy)_2P(\mu\text{-}NCy)(\mu\text{-}NSiMe_3)]AlMe_2$} (5a).

The reaction of $(^tBuNH)_3PNSiMe_3$ (**3a**) with trimethylaluminum in a 1:1 molar ratio results in the elimination of one equivalent of methane and the formation of {$Me_2Al[(\mu\text{-}N^tBu)(\mu\text{-}NSiMe_3)P(NH^tBu)_2]$} (**4**) in good yield. On the basis of NMR data complex **4** is assigned a monocyclic structure in which the aluminum center is chelated

by the two imido groups (N^tBu and $NSiMe_3$) of the monoanionic ligand (formally isoelectronic with $[H_2PO_4]^{2-}$), while the two NH^tBu groups are in exocyclic positions. The ^1H NMR spectrum of **4** in C_6D_6 contains two ^{t}Bu resonances at 1.16 and 1.29 ppm (relative intensities 2:1), attributed to the NH^tBu and N^tBu groups, respectively. Resonances due to the $SiMe_3$ and $AlMe_2$ units with the appropriate intensities are observed at 0.34 and -0.22 ppm, respectively. The ^{13}C NMR spectrum of **4** exhibits resonances for two types of ^{t}Bu groups, one $SiMe_3$ group and an $AlMe_2$ unit, consistent with this structural proposal; the ^{31}P spectrum reveals a singlet at 5.6 ppm. Single crystals of **4** could not be obtained owing to its high solubility in organic solvents.

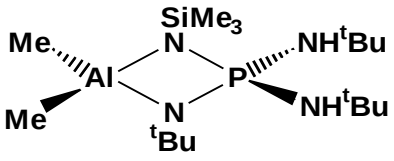

4

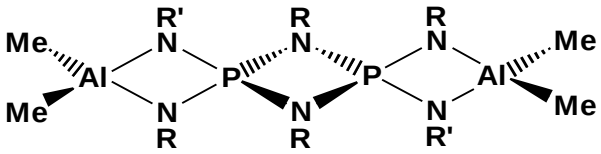

5

Interestingly, the reaction of the cyclohexyl derivative $(CyNH)_3PNSiMe_3$ (**3b**) with $AlMe_3$ proceeds in a different manner. In this case elimination of an equivalent of cyclohexylamine results in the nearly quantitative formation of $\{Me_2Al[(\mu\text{-}NCy)(\mu\text{-}NSiMe_3)P(\mu\text{-}NCy)_2P(\mu\text{-}NCy)(\mu\text{-}NSiMe_3)]AlMe_2\}$ (**5a**). An X-ray structure of **5a** revealed a centrosymmetric dimer in which the central feature is an essentially planar P_2N_2 ring with the two phosphorus atoms are linked by NCy groups (Figure 1). Complex **5a** is the dimethylaluminum derivative of the trisimidometaphosphate monoanion $[P(NCy)_2(NSiMe_3)]^-$. Two closely related complexes have been isolated by Stahl *et al.*[4c] from the reaction of the bis(amino)-cyclodiphosph(V)azanes *cis*-$\{(^tBuNH)(RN{=}PN^tBu)_2(NH^tBu)\}$ with trimethylaluminum. The general structure of

these tricyclic species is shown above (**5a**, R = Cy, R' = $SiMe_3$; **5b**, R = ^tBu, R' = Ph; **5c**, R = ^tBu, R' = *p*-tol).

Selected bond lengths and bond angles of **5a** are shown in Table 2. Each phosphorus atom is also part of a planar four-membered PN_2Al ring that is approximately perpendicular to the P_2N_2 ring. The dimethylaluminum cations are chelated by an $NSiMe_3$ group and the NCy group that is not involved in the central P_2N_2 ring. The P-N distances involving these two imido ligands are very similar [P(1)-N(1) = 1.5903(15) Å; P(1)-N(2) = 1.5952(15) Å] despite their different substituents. These bond lengths are significantly shorter than those in the P_2N_2 ring [P(1)-N(3) = 1.6816(16) Å] indicating a higher formal bond order in the former. The two Al-N bond lengths also differ slightly [Al(1)-N(1) = 1.9597(16) Å; Al(1)-N(2) = 1.9251(16) Å], with the shorter bond observed in the case of the more basic NCy ligand.

A comparison of structural parameters of **5a** and **5c**[4c] shows the expected similarities, with P-N single bond distances of 1.701(2) Å observed within the P_2N_2 ring of **5c** [*c.f.* 1.6816(16) Å in **5a**], and the Al-N distances in **5a** [avg. = 1.942(2) Å] slightly shorter than the average bond length in **5c** [1.958(2) Å]. Conversely, longer Al-C distances are observed in **5a** [1.961(2) Å] than in **5c** [1.944(2) Å]. These minor differences can be attributed to the more electron-donating character of the cyclohexylimido substituents of **5a** as compared to the NR (R = ^tBu, *p*-tol) groups of **5c**.

The NMR spectra of **5a** in C_6D_6 are consistent with the retention of its dimeric structure in solution. In particular, the ^{13}C NMR spectrum contained two sets of cyclohexyl resonances as well as signals attributed to the $SiMe_3$ (2.67 ppm) and $AlMe_2$ (-6.81 ppm) fragments. The ^{31}P NMR signal for **5a** appears at 17.1 ppm. While the yields

involved in the two-step syntheses of the imidometaphosphate dimers **5b** and **5c** range from moderate to excellent,[4c, 24] the preparation of **5a** requires only one step and does not involve the use of potentially explosive organic azides.

Synthesis and NMR Characterization of {$Me_2Al[(\mu\text{-}S)(\mu\text{-}N^tBu)P(NH^tBu)_2]$} (7) and {$Me_2Al[(\mu\text{-}S)(\mu\text{-}N^tBu)P(\mu\text{-}NH^tBu)(\mu\text{-}N^tBu)]AlMe_2$} (8).

In earlier attempts[8] to prepare a trisimido(thio)phosphate trianion $[SP(NR)_3]^{3-}$, it was found that the reaction of $SP(NH^tBu)_3$ (**2a**) with two equivalents of *n*-butyllithium results in the extrusion of sulfur and the formation of the cubic tris(imido)metaphosphate dimer $\{[\mu_3\text{-}Li(THF)][P(\mu_3\text{-}N^tBu)_2(N^tBu)]\}_2$ (**6**) in 15 % yield. In light of the results described earlier, investigations into the reactions of trisamino(thio)phosphates $SP(NHR)_3$ (**2**) with $AlMe_3$ are of considerable interest, as three possible reaction pathways can be envisioned: (i) monodeprotonation of **2** to yield a $[Me_2Al]^+$ complex of the $[SP(NR)(NHR)_2]^-$ anion, (ii) deprotonation and loss of RNH_2 to yield a bis(imido)(thio)metaphosphate $[SP(NR)_2]^-$ monoanion, or (iii) deprotonation and sulfur extrusion to generate a tris(imido)metaphosphate $[P(NR)_3]^-$ complex.

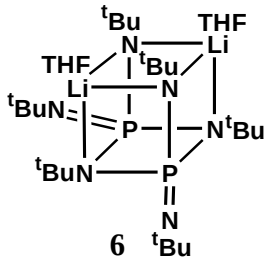

6

The reaction of $SP(NH^tBu)_3$ (**2a**) with one equivalent of $AlMe_3$ results in the formation of **7**, a white powder, which has been characterized by multinuclear NMR spectroscopy. The ^{31}P NMR spectrum of the product in C_6D_6 contained a single

resonance at 35.6 ppm (*c.f.* 46.3 ppm for **2a**), a strong indication that loss of sulfur has not occurred, since this would be accompanied by a significant upfield shift as is observed for **6** (^{31}P NMR: -21 ppm).[8] The ^{1}H NMR spectrum displayed two *tert*-butyl signals at 1.23 and 1.18 ppm in a 1:2 ratio, along with a peak at -0.24 ppm attributed to a Me_2Al^+ cation; the corresponding signals were observed in the ^{13}C NMR spectrum. These NMR data are consistent with the formation of {$Me_2Al[(\mu\text{-}S)(\mu\text{-}N^tBu)P(NH^tBu)_2]$} (**7**), a monocyclic species which is isostructural with **4** and, like **4**, is the product of a simple deprotonation reaction.

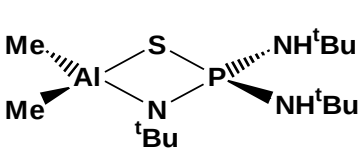

7

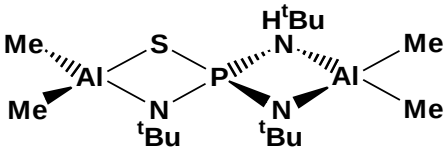

8

The reaction of **2a** with two equivalents of $AlMe_3$ yields a white powder which has been identified as the spirocyclic complex {$Me_2Al[(\mu\text{-}S)(\mu\text{-}N^tBu)P(\mu\text{-}NH^tBu)(\mu\text{-}N^tBu)]AlMe_2$} (**8**) based on multinuclear NMR data. A single ^{31}P resonance was observed at 40.9 ppm, indicating that the P-S bond remains intact (*vide supra*). The ^{1}H NMR spectrum in C_6D_6 contained three *tert*-butyl resonances of equal intensities, as well as four signals between -0.54 and -0.25 ppm attributed to the methyl groups of the two inequivalent dimethylaluminum cations. The corresponding ^{t}Bu signals were observed in the ^{13}C NMR spectrum, along with two broad resonances assigned to the Me_2Al^+ cations. The fact that the four methyl groups resonate at different ^{1}H NMR frequencies is attributed to the lack of planarity in both the AlSNP and AlN_2P rings, resulting in a molecule with only C_1 symmetry.

Further investigations of the reaction of **2a** with $AlMe_3$ as a function of stoichiometry, reaction time, and reaction temperature, did not yield any products other than **7** and **8**. Similarly, attempts to form a methylaluminum complex of the amidotris(imido)phosphate dianion $[P(NH^tBu)(N^tBu)_2(NSiMe_3)]^{2-}$ by increasing the reaction time and temperature or changing the stoichiometry of the reagents were not successful; in all cases, only **4** was obtained. The nearly quantitative formation of the simple dimethylaluminum derivatives **4**, **7**, and **8** is in sharp contrast to our observations for the reactions of $OP(NH^tBu)_3$ (**1**) with $AlMe_3$ in which products involving monoanionic and dianionic ligands, as well as the neutral ligand **1**, were obtained.[12]

Synthesis and NMR Characterization of {$Me_2Al[(\mu\text{-}N^tBu)(\mu\text{-}NSiMe_3)P(\mu\text{-}NH^tBu)(\mu\text{-}N^tBu)]Li(THF)_2$} (9a•2THF), {$[Me_2Al][Li]_2[P(N^tBu)_3(NSiMe_3)]$} (10) and {$Me_2Al[(\mu\text{-}N^tBu)_2P(\mu_2\text{-}N^tBu)_2(\mu_2\text{-}THF)][Li(THF)]_2$} (11a); X-ray Structures of (9a•2THF) and (11a).

In view of the limited reactivity of $AlMe_3$ towards $(^tBuNH)_3PNSiMe_3$ (**3a**), deprotonation of the dimethylaluminum complex **4** with ^nBuLi was investigated. The treatment of **4** with one equivalent of ^nBuLi resulted in the isolation of the heterobimetallic complex $\{[Me_2Al][Li][P(N^tBu)_2(NH^tBu)(NSiMe_3)]\}$ (**9a**) in essentially quantitative yield. Recrystallization of **9a** from THF/hexane produced colorless crystals of **9a**•2THF; an X-ray structure (Figure 2) revealed that this complex exists as the spirocycle $\{Me_2Al[(\mu\text{-}N^tBu)(\mu\text{-}NSiMe_3)P(\mu\text{-}NH^tBu)(\mu\text{-}N^tBu)]Li(THF)_2\}$ in which the dimethylaluminum cation is *N,N'*-chelated by the $NSiMe_3$ group and one N^tBu unit, while the lithium cation is coordinated to the remaining N^tBu and NH^tBu groups, and to two

molecules of tetrahydrofuran. Pertinent bond lengths and angles are given in Table 3, and are in good agreement with metrical parameters calculated for the model system $\{Me_2Al[(\mu\text{-}NMe)(\mu\text{-}NSiH_3)P(\mu\text{-}NHMe)(\mu\text{-}NMe)]Li(OMe_2)_2\}$ (**9b**•2OMe_2) particularly when the difference in the identities of the imido groups is taken into account.

The P-N distances in **9a**•2THF range from 1.588(3) Å to 1.716(3) Å, with identical bond lengths of 1.640(4) Å observed for the two nitrogen atoms that chelate the aluminum centre. A longer P-N distance is present between the phosphorus and the *tert*-butylamido nitrogen [1.716(3) Å], while a significantly shorter distance is found for the P=N^{t}Bu bond [1.588(3) Å], indicating the presence of localized single and double bonds phosphorus-nitrogen bonds for N(4) and N(3), respectively. The mean Al-N distances in **9a**•2THF [1.899(4) Å] are slightly shorter than those observed in **5a** [1.9422(2) Å], presumably due to the larger formal charge on each of the chelating imido groups of **9a**•2THF as compared to those of **5a**. As expected, the Li-N bond to the monanion NH^{t}Bu ligand [2.178(7) Å] is substantially longer than the Li-N linkage involving the dianionic N^{t}Bu ligand [1.969(7) Å]. The angles about these two nitrogen atoms are also significantly different [∠PN(3)Li = 100.6(3)°; ∠PN(4)Li 88.9(2)°] due to their different hybridizations. In consequence, while the four-membered AlN_2P ring is essentially planar [∠N(1)Al(1)N(2)P(1) = -1.15(15)°], the LiN_2P ring is puckered [∠N(4)P(1)N(3)Li(1) = 17.9(3)°]. This X-ray structure confirmed the coordination mode of the ligand to the $AlMe_2$ unit of **4** that was deduced from the NMR data (*vide supra*).

The ^{1}H NMR spectrum of **9a** in d_8-THF contains three ^{t}Bu signals of equal intensities at 1.35, 1.31, and 1.29 ppm, as well as a single $SiMe_3$ resonance at 0.13 ppm and a singlet at -0.89 ppm due to the two equivalent methyl groups of the $AlMe_2$ unit.

The corresponding signals were observed in the ^{13}C NMR spectrum, while a single resonance at 8.2 ppm was observed in the ^{31}P NMR spectrum. These spectroscopic data are consistent with the retention of the spirocyclic structure of **9a**•2THF in THF solution.

In a similar manner, the dilithiated complex {[Me_2Al][Li]$_2$[$P(N^tBu)_3(NSiMe_3)$]} (**10**) is recovered in excellent yield from the reaction of **4**, prepared *in situ*, with two equivalents of ^{n}BuLi (Scheme 1). An analogous synthesis of the symmetrical tetraimidophosphate trianion $[P(N^tBu)_4]^{3-}$ as the heterobimetallic complex {[Me_2Al][Li]$_2$[$P(N^tBu)_4$]} was carried out by treating (^{t}BuNH)$_3$PN^tBu first with $AlMe_3$, then with ^{n}BuLi. The structure of the THF adduct {Me_2Al[(μ-N^tBu)$_2$P(μ$_2$-N^tBu)$_2$(μ$_2$-THF)][Li(THF)]$_2$} (**11a**) was determined by X-ray crystallography. This complex crystallizes with a molecule of THF in its lattice, rendering the crystals unstable toward solvent loss once removed from solution. Consequently, the X-ray data are not of sufficient quality to allow for a discussion of the bond lengths and angles of this compound. However, the structural parameters are consistent with the corresponding parameters which were calculated for the model system {Me_2Al[(μ-NMe)$_2$P(μ$_2$-NMe)$_2$(μ$_2$-OMe_2)[Li(OMe_2)]$_2$} (**11b**) (Table 4).

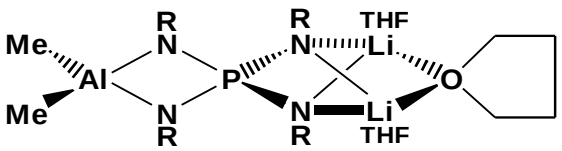

11

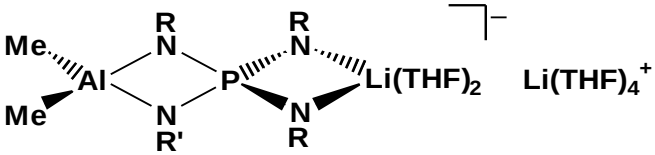

12

Complexes **10** and **11a** have been characterized by multinuclear (^1H, ^7Li, ^{13}C, and ^{31}P) NMR spectroscopy. The ^1H NMR spectrum of **10** in d_8-THF consists of two ^{t}Bu signals in a 1:2 ratio at 1.32 and 1.30 ppm, as well as singlets at 0.08 ppm and -0.94 ppm attributed to the $SiMe_3$ and $AlMe_2$ groups, respectively; the corresponding signals are

observed in the ^{13}C NMR spectrum. While the expected singlet is observed at 10.0 ppm in the ^{31}P NMR spectrum, two resonances of approximately equal intensities are present in the ^{7}Li NMR spectrum at 1.44 and –2.71 ppm. The latter observation suggests that, in THF solution, solvation of one lithium cation occurs to produce the solvent-separated ion pair $\{[Li(THF)_4]\}^+\{Me_2Al[(\mu\text{-}N^tBu)(\mu\text{-}NSiMe_3)P(\mu\text{-}N^tBu)_2]Li(THF)_2\}^-$ (**12**), comprised of a spirocyclic monoanion and a tetrasolvated lithium counterion. The related tetra(naphthylimido)phosphate $\{[Li(THF)_4]\}^+\{Li(THF)_2[(\mu\text{-}Nnaph)_2P(\mu\text{-}Nnaph)_2]Li(THF)_2]\}^-$ is known to have a spirocyclic structure in the solid state.[5]

In contrast, the NMR data obtained for **11a** in d_8-THF are consistent with its solid-state structure. The inequivalence of the two types of *tert*-butyl groups is not apparent from the ^{1}H NMR spectrum, since only a single ^{t}Bu resonance (1.34 ppm) is observed, accompanied by a singlet at -0.96 ppm attributed to the Me_2Al group. However, the ^{13}C NMR spectrum clearly shows two sets of ^{t}Bu signals (50.90 and 36.41 ppm; 50.78 and 34.45 ppm) with approximately equal intensities. The ^{7}Li NMR spectrum exhibits a singlet at 1.23 ppm indicating the equivalence of the two lithium cations and thus that formation of a solvent-separated ion pair does not occur for **11a**.

Reactions of **3a** with $AlMe_3$ and $^{n}BuLi$ in THF are readily monitored by ^{31}P NMR spectroscopy, as a down-field shift is observed with each subsequent deprotonation of the ligand. The signal at -15 ppm for $(^{t}BuNH)_3PNSiMe_3$ disappears as the dimethylaluminum complex **4** forms (5.6 ppm). Initially, the addition of $^{n}BuLi$ results in the appearance of a peak at 8.2 ppm (**9a**); as more *n*-butyllithium is added, a signal for the dilithiated complex **12** is observed at 10.0 ppm. A similar trend in ^{31}P NMR chemical

shifts is observed when **3a** is reacted with one, two, and three equivalents of *n*-butyllithium.[11]

EPR and DFT Characterization of the Persistent Radicals {$Me_2Al[(\mu\text{-}NR)(\mu\text{-}N^tBu)P(\mu\text{-}N^tBu)_2]Li(THF)_2\}^{\bullet}$ (13a, R = $SiMe_3$; 14a, R = ^{t}Bu)

When exposed to air, THF solutions of **12** turn a bright blue color, while solutions of **11a** become a deep teal color indicative of the formation of radicals. In earlier studies, we have isolated stable cubic tetraimidophosphate radicals by oxidization of the dimeric lithium salt $\{Li_3[P(N^tBu)_3(NSiMe_3)]\}_2$ with one equivalent of iodine or bromine.[25] Oxidations of the dimethylaluminum complexes **11a** and **12** are expected to yield neutral spirocyclic radicals via the elimination of one equivalent of THF-solvated lithium halide (Scheme 1). In practice, addition of a half-equivalent of iodine to a colorless solution of **12** in THF results in an intense blue color, which persists for several hours in solution. In the solid state, this mixed heterobimetallic tetraimidophosphate radical **13a** is stable for only a few minutes; however, it has been identified by its solution EPR spectrum (Figure 3). The observed pattern is primarily a doublet due to coupling of the unpaired electron to the phosphorus atom (^{31}P, 100 %, I = 1/2), with a total of approximately 50 lines due to additional hyperfine coupling to the nitrogen (^{14}N, 99 %, I = 1), lithium (^{7}Li, 92.5 %, I = 3/2), and aluminum (^{27}Al, 100 %, I = 5/2) nuclei.

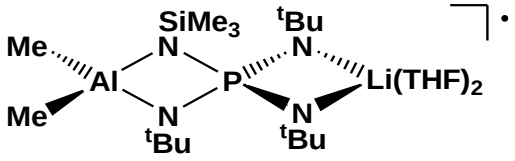

13a

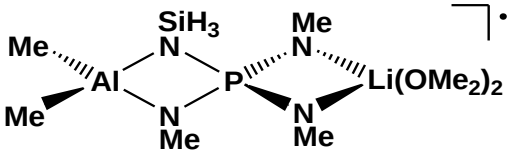

13b

To aid in the interpretation of this complex spectrum, the model system $\{Me_2Al[(\mu\text{-}NMe)(\mu\text{-}NSiH_3)P(\mu\text{-}NMe)_2]Li(Me_2O)_2\}^{\bullet}$ (**13b**) was examined by means of

DFT calculations. The optimized molecular structure displays C_s symmetry, with the AlN_2P and LiN_2P rings perpendicular to one another. The two NMe groups that chelate the lithium cation have equivalent P-N bond lengths of 1.668 Å, while slightly shorter P-N bond distances are observed for the remaining P-NMe unit (1.655 Å) and the $P\text{-}NSiH_3$ (1.650 Å) fragment. The four metal-nitrogen distances are quite similar, with an average N-Al bond length of 1.958 Å and identical Li-N distances (2.030 Å).

Single point calculations on **13b** indicated that the singly occupied molecular orbital (SOMO) is primarily a linear combination of nitrogen *p*-orbitals (Figure 4). For symmetry reasons, the contributions from the nitrogen atoms in the AlN_2P and LiN_2P rings are not equivalent; a Mulliken population analysis of the atomic spin densities revealed that the spin density is concentrated on the nitrogen atoms of the LiN_2P ring. Although the SOMO has only minor contributions from phosphorus, lithium and aluminium, these atoms have non-zero spin densities owing to spin polarization effects. In consequence, the EPR spectrum of **13b**, and hence that of its parent system **13a**, is expected to show large hyperfine couplings to one phosphorus and two equivalent nitrogen atoms. Smaller couplings to the other two nitrogen atoms and the metal centers should also be present, and are responsible for the extensive hyperfine structure seen in the experimental EPR spectrum. While the calculations indicate that the Me_2Al^+ cation also contributes to the SOMO, coupling to the methyl protons is expected to be so small as to be unobservable.

An excellent simulation of the experimental EPR spectrum was obtained by including hyperfine couplings to one phosphorus atom (29.29 G), one lithium cation (1.43 G) and one aluminum atom (1.39 G), a pair of equivalent nitrogen nuclei (7.20 G),

and two unique nitrogen atoms (1.61 G and 0.27 G) (Figure 3). These hyperfine couplings are consistent with the retention of the spirocyclic arrangement of **12** upon oxidation and the formation of the neutral radical $\{Me_2Al[(\mu\text{-}N^tBu)_2P(\mu\text{-}N^tBu)_2]Li(THF)_2\}^{\bullet}$ (**13a**) (Scheme 1). In order to confirm the relative magnitudes of the HFCCs used to create the spectral simulation, the calculated data for **13b** were examined more closely. The differing spin densities on the nitrogen atoms are reflected in the ^{14}N hyperfine coupling constants, which were calculated to be largest for the two equivalent N^tBu ligands which chelate the lithium cation (6.61 G), smallest for the $NSiMe_3$ group (-0.07 G), and of an intermediate size for the unique N^tBu nitrogen atom (-1.29 G). The calculated hyperfine coupling constants are shown in Table 5, along with the values used to create the spectral simulation shown in Figure 3. The largest calculated HFCC was to the phosphorus nucleus (-30.72 G), while the much smaller aluminum (-1.22 G) and lithium (-1.67 G) couplings are calculated to be fairly similar. These calculated HFCCs provide good support for the proposed spirocyclic structure of the radical **13a**.

The one-electron oxidation of **11a** with halogens yields the persistent teal radical $\{Me_2Al[(\mu\text{-}N^tBu)_2P(\mu\text{-}N^tBu)_2]Li(THF)_2\}^{\bullet}$ (**14a**) with a similar stability to that of **13a**: it persists in solution for approximately 3 h, but cannot be isolated in the solid state. The solution EPR spectrum of this radical is shown in Figure 5. DFT calculations were carried out on the model system $\{Me_2Al[(\mu\text{-}NMe)_2P(\mu\text{-}NMe)_2]Li(Me_2O)_2\}^{\bullet}$ (**14b**). The geometry-optimized structure of this molecule has C_{2v} symmetry, with the two MN_2P (M = Li, Al) rings perpendicular to one another. The two pairs of P-N bond lengths in this structure are equivalent within the accuracy of the calculations, at 1.650 Å and 1.653 Å

for the P-N-Al and P-N-Li distances, respectively. As was seen for **13b**, the Al-N bonds (1.936 Å) are slightly shorter than are the Li-N bonds (1.984 Å).

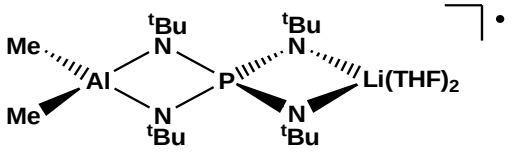

14a

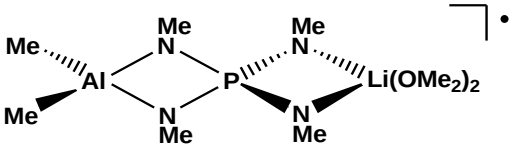

14b

Further examination of the data indicated that the composition of the SOMO (Figure 4) of **14b** is similar to that of **13b**. An excellent simulation of the experimental EPR spectrum was obtained by including hyperfine couplings to two pairs of equivalent ^{14}N atoms (6.44 G; 1.67 G), one lithium cation (1.40 G), one dimethylaluminum cation (1.99 G), and the phosphorus atom (28.45 G). The close agreement of the experimental and calculated HFCs, which are shown in Table 5, confirms that the oxidation product of **11a** is indeed the neutral spirocycle radical $\{Me_2Al[(\mu\text{-}N^tBu)_2P(\mu\text{-}N^tBu)_2]Li(THF)_2\}^{\bullet}$ (**14a**). Unlike other related tetraimidophosphate radicals,[25] the EPR spectra of **13a** and **14a** are not dependent on sample concentration, indicating that dissociation of these spirocyclic radicals (*e.g.* by solvation of the lithium cations) does not occur even in very dilute solutions.

Synthesis and Characterization of $\{Mg[(\mu\text{-}N^tBu)(\mu\text{-}NH^tBu)P(NH^tBu)(NSiMe_3)]_2\}$ (15), $\{Mg[(\mu\text{-}NCy)(\mu\text{-}NSiMe_3)P(NHCy)_2]_2\}$ (16), $\{Mg[(\mu\text{-}S)(\mu\text{-}N^tBu)P(NH^tBu)_2]_2\}$ (17), and $\{[MgOH][(\mu\text{-}S)(\mu\text{-}N^tBu)P(NH^tBu)_2]\}_6$ (18).

The reaction of $MgBu_2$ with two equivalents of $(^tBuNH)_3PNSiMe_3$ (**3a**) produces a complex in which a magnesium dication is bis-chelated by two imidophosphate monoanions $\{Mg[(\mu\text{-}N^tBu)(\mu\text{-}NH^tBu)P(NH^tBu)(NSiMe_3)]_2\}$ **15**. This compound has

been characterized by multinuclear NMR spectroscopy, and displays a single resonance in its ^{31}P spectrum at 5.2 ppm. The ^{1}H NMR spectrum of **15** in C_6D_6 is interesting in that it consists of three ^{t}Bu signals of equal intensities, one $SiMe_3$ resonance, and two broad doublets which are attributable to two inequivalent NH protons. These data indicate that the imidophosphate ligand is coordinated to the magnesium atom through one $NH^{t}Bu$ and one $N^{t}Bu$ group. This is somewhat surprising, considering the well-established structures of the dimethylaluminum complexes **4**, **9a**, **10**, and **11a**, in which the aluminum atom is chelated by the two imido groups, while the amido substituents remain non-coordinated. This preference is attributed to the fact that Mg^{2+} is a harder acid than Me_2Al^{+} and will, therefore, prefer coordination to the harder base $NH^{t}Bu$ over coordination to the $NSiMe_3$ nitrogen atom.

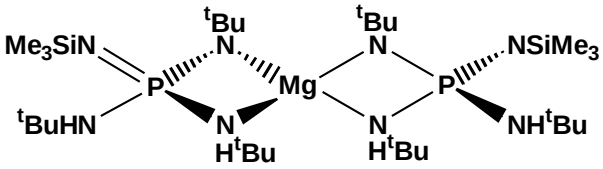

15

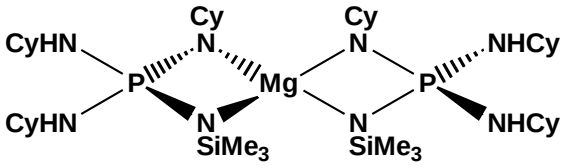

16

The reaction of $MgBu_2$ with the cyclohexyl derivative $(CyNH)_3PNSiMe_3$ (**3b**) in a 1:2 molar ratio produces a complex that was identified as $\{Mg[(\mu\text{-}NCy)(\mu\text{-}NSiMe_3)P(NHCy)_2]_2\}$ (**16**) on the basis of NMR data and CHN analysis. The appearance of resonances for only two cyclohexyl environments in a 2:1 ratio in the ^{13}C NMR spectrum (in C_6D_6) suggests coordination of two imido groups ($NSiMe_3$ and NCy) to the magnesium center and two exocyclic cyclohexylamido groups.

Attempts to effect further deprotonation by changing the reaction conditions and stoichiometry were unsuccessful; the only products observed by ^{31}P NMR were the monoanionic complexes **15** and **16**. Similar low reactivities were observed for these

species towards dimethylzinc and trimethylaluminum. However, the trisamino(thio)phosphate $SP(NH^tBu)_3$ (**2a**) was previously found to be slightly more reactive than $(RNH)_3PNSiMe_3$ towards $ZnMe_2$.[7] Consequently, reactions between $MgBu_2$ and **2a** were explored using various stoichiometries and reaction conditions.

When a half-equivalent of $MgBu_2$ was employed, a white powder was recovered which gave rise to only one ^{31}P NMR signal (38.8 ppm). The ^1H NMR and ^{13}C NMR spectra of the product in C_6D_6 indicated the presence of two inequivalent ^{t}Bu environments. The 1:2 integration of the ^1H NMR peaks (at 1.56 ppm and 1.45 ppm), and the absence of any resonances attributable to a $BuMg^+$ cation, is consistent with the formation of the *N*,*S*-chelated complex $\{Mg[(\mu\text{-}S)(\mu\text{-}N^tBu)P(NH^tBu)_2]_2\}$ (**17**).

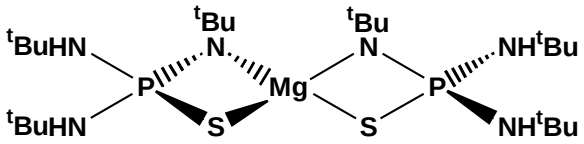

17

Attempts to grow single crystals of **17** from a variety of organic solvents were unsuccessful; however, it was found that prolonged storage of this complex in Et_2O leads to the of the hexameric complex $\{[Mg\mu_3\text{-}OH][(\mu\text{-}S)(\mu\text{-}N^tBu)P(NH^tBu)_2]\}_6$ (**18**), presumably via the partial hydrolysis of **17**. An X-ray structure of **18** (Figure 6) revealed that the core of this complex is composed of six $[Mg\mu_3\text{-}OH]^+$ cations linked together via Mg-O bonds to form two stacked six-membered Mg_3O_3 rings (or a Mg_6O_6 hexagonal prism). Each magnesium center is also *N*,*S*-chelated by the monoanionic ligands $[SP(NH^tBu)_2(N^tBu)]^-$, rendering the Mg^{2+} cations pentacoordinate. The bis(amido)imido(thio)phosphate ligands radiate outwards from the Mg_6O_6 core, with the two ^{t}BuNH groups of each ligand remaining non-coordinated. Selected bond lengths and

bond angles for **18** are summarized in Table 6. The three Mg-O bonds in the center of the molecule are inequivalent: each magnesium atom has one short bond [e.g. Mg(1)-O(3) = 2.0030(16) Å], which can be considered a discrete $[MgOH]^+$ unit, one slightly weaker bond [Mg(1)-O(1) = 2.0266(15) Å] to a second oxygen atom within a Mg_3O_3 ring, and a third, longer distance [Mg(1)-O(2) = 2.1191(15) Å] between the magnesium of one Mg_3O_3 ring and an oxygen atom in the other six-membered ring. The average Mg-O bond distance in **18** is 2.054(15) Å, *c.f.* 1.9473(13)-2.0020(14) Å for the related complex $\{[NaMg(N^iPr)_2(O)\bullet THF\}_6$ which also contains a core of two stacked Mg_3O_3 rings.[26] The bis(amido)imido(thio)phosphate ligand, as expected, contains one short P-N bond to the *tert*-butylimido nitrogen atom [P(1)-N(1) =1.6078(16) Å], while longer distances are observed to the two *tert*-butylamido groups [P(1)-N(2) =1.6532(17) Å; P(1)-N(3) = 1.6721(18) Å].

The deliberate hydrolysis of **17** with one equivalent of H_2O was attempted in both diethyl ether and toluene. Reaction times of more than 10 min result in the complete hydrolysis of **17**, and a mixture of $SP(NH^tBu)_3$ (**2a**) and magnesium oxide was recovered. Over shorter reaction times, two signals of equal intensities attributable to **2a** and **17** are observed in the ^{31}P NMR spectrum of the product mixture. It is thought that removal of the solvent under vacuum facilitates the loss of water from **18** so that the hydroxide complex is not observed.

The reaction of **2a** and $MgBu_2$ in a 1:1 stoichiometry gave a complex mixture of products, as revealed by ^{31}P NMR spectra. The marked increase in the number of products formed from the reaction of $EP(NH^tBu)_3$ (E = O, S) with dibutylmagnesium as compared to dimethylzinc[7] can be attributed to the higher electrophilicity of the

magnesium cations, and their tendency to adopt octahedral rather than tetrahedral coordination modes.

Conclusions

The trisamidophosphates $EP(NHR)_3$ (E = O, S, NR'; R = alkyl) display similar reactivities toward $AlMe_3$ as they do toward $ZnMe_2$, with the highest reactivity observed for E = O, and the lowest reactivity for E = NR'. Three-fold deprotonation of these species to form imido analogues of the well-known aluminophosphates does not occur. In the case of E = NR', two different reaction pathways can occur to yield imido analogues of ortho- or meta-phosphate, depending on the identity of the R group employed. Reactions of $AlMe_3$ with $SP(NH^tBu)_3$ yield *N*,*S*-chelated complexes Lithiation of aluminum bis(amido)bis(imido)phosphates produces heterobimetallic complexes which form persistent radicals upon oxidation with iodine. Reactions with $MgBu_2$ lead to multiple products for E = O, S, but only a simple monoanionic complex of E = NR'. The different behaviors of **1**-**3** toward various organometallic (metal alkyl) reagents are summarized in Table 7.

Acknowledgments

We thank the University of Calgary and the Natural Sciences and Engineering Research Council of Canada for funding, and Helsingin Sanomain 100-vuotissäätiö for a scholarship (H. M. T.).

Supporting Information Available: Crystallographic *.cif files are included in the Supporting Information. This material is available free of charge via the Internet at http://pubs.acs.org.

References

(1) For recent reviews, see (a) Brask, J. K.; Chivers, T. *Angew. Chem. Int. Ed.* **2001**, *40*, 3960-3976; (b) Aspinall, G. M.; Copsey, M. C.; Leedham, A. P.; Russell, C. A. *Coord. Chem. Rev.* **2002**, *227*, 217-232.

(2) The original definition of "isoelectronic" (isosteric) compounds restricts the term to species having the *same number of atoms* and the same number of electrons (Langmuir, I. *J. Am. Chem. Soc.* **1919**, *41*, 1543). Thus, according to this definition, N^{3-} is isoelectronic with O^{2-}. However, nitrides are compositionally different to oxides as a result of the different charges on the anions.

(3) Chivers, T. *Top. Curr. Chem.* **2003**, *229*, 143-159.

(4) See, for example, (a) Niecke, E.; Frost, M.; Nieger, M.; von der Gönna, V.; Ruban, A.; Schoeller, W. W. *Angew. Chem. Int. Ed.* **1994**, *33*, 2111. (b) Scherer, O. J.; Quintus, P.; Kaub, J.; Sheldrick, W. S. *Chem. Ber.* **1987**, *120*, 1463. (c) Lief, G. R.; Carrow, C. J.; Stahl, L.; Staples, R. J. *Organometallics* **2001**, *20*, 1629.

(5) Raithby, P. R., Russell, C. A., Steiner, A., Wright, D. S. *Angew. Chem. Int. Ed.* **1997**, *36*, 649-650.

(6) Armstrong, A.; Chivers, T.; Krahn, M.; Parvez, M.; Schatte, G. *Chem. Commun.* **2002**, 2332-2333.

(7) Armstrong, A.; Chivers, T.; Krahn, M.; Parvez, M. *Can. J. Chem.*, submitted.

(8) Chivers, T.; Krahn, M.; Schatte, G.; Parvez, M. *Inorg. Chem.* **2003**, 42, 3994-4005.

(9) Rufanov, K. A.; Ziemer, B.; Meisel, M. *Dalton Trans.* **2004**, 3808-3809.

(10) Chivers, T.; Krahn, M.; Parvez, M.; Schatte, G. *Chem. Commun.* **2001**, 1992-1993.

(11) Armstrong, A.; Chivers, T.; Parvez, M.; Boeré, R. T. *Inorg. Chem.* **2004**, *43*, 3453-3460.

(12) Blais, P.; Chivers, T.; Krahn, M.; Schatte, G. *J. Organomet. Chem.* **2002**, *646*, 107-112.

(13) For a recent review, see Kimura, T. *Micropor. Mesopor. Mater.* **2005**, *77*, 97-107.

(14) Eloranta, J. *XEMR* version 0.7, University of Jyväskylä, Finland.

(15) Bruker Analytische Messtechnik GmbH, *WINEPR SimFonia* version 1.25 **1996**.

(16) Altomare, A.; Cascarano, M.; Giacovazzo, C.; Guagliardi, A. *J. Appl. Cryst*., **1993**, *26*, 343.

(17) Sheldrick, G. M. *SHELXL-97, Program for the Solution of Crystal Structures* **1997**, University of Göttingen, Germany.

(18) (a) Perdew, J. P.; Burke, K.; Ernzerhof, M. *Phys. Rev. Lett.* **1996**, *77*, 3865-3868; (b) Perdew, J. P.; Burke, K.; Ernzerhof, M. *Phys. Rev. Lett***. 1997**, *78*, 1396-1396 (E).

(19) Perdew, J. P.; Ernzerhof, M.; Burke, K. *J. Chem. Phys.* **1996**, *105*, 9982-9985.

(20) The TZVP basis set was used as it is referenced in the Turbomole 5.7 internal basis set library.

(21) The basis set was taken from EMSL basis set library: http://www.emsl.pnl.gov/forms/basisform.html. Site accessed December 2004.

(22) TURBOMOLE, Program Package for *ab initio* Electronic Structure Calculations, Version 5.7. R. Ahlrichs, *et al.* Theoretical Chemistry Group, University of Karlsruhe, Karlsruhe, Germany, 2004.

(23) Gaussian 03, Revision C.02, Frisch, M. J.; Trucks, G. W.; Schlegel, H. B.; Scuseria, G. E.; Robb, M. A.; Cheeseman, J. R.; Montgomery, Jr., J. A.; Vreven, T.; Kudin, K. N.; Burant, J. C.; Millam, J. M.; Iyengar, S. S.; Tomasi, J.; Barone, V.; Mennucci, B.; Cossi, M.; Scalmani, G.; Rega, N.; Petersson, G. A.; Nakatsuji, H.; Hada, M.; Ehara, M.; Toyota, K.; Fukuda, R.; Hasegawa, J.; Ishida, M.; Nakajima, T.; Honda, Y.; Kitao, O.; Nakai, H.; Klene, M.; Li, X.; Knox, J. E.; Hratchian, H. P.; Cross, J. B.; Bakken, V.; Adamo, C.; Jaramillo, J.; Gomperts, R.; Stratmann, R. E.; Yazyev, O.; Austin, A. J.; Cammi, R.; Pomelli, C.; Ochterski, J. W.; Ayala, P. Y.; Morokuma, K.; Voth, G. A.; Salvador, P.; Dannenberg, J. J.; Zakrzewski, V. G.; Dapprich, S.; Daniels, A. D.; Strain, M. C.; Farkas, O.; Malick, D. K.; Rabuck, A. D.; Raghavachari, K.; Foresman, J. B.; Ortiz, J. V.; Cui, Q.; Baboul, A. G.; Clifford, S.; Cioslowski, J.; Stefanov, B. B.; Liu, G.; Liashenko, A.; Piskorz, P.; Komaromi, I.; Martin, R. L.; Fox, D. J.; Keith, T.; Al-Laham, M. A.; Peng, C. Y.; Nanayakkara, A.; Challacombe, M.; Gill, P. M. W.; Johnson, B.; Chen, W.; Wong, M. W.; Gonzalez, C.; Pople, J. A.; Gaussian, Inc., Wallingford CT, 2004.

(24) Moser, D. F.; Carrow, C. J.; Stahl, L.; Staples, R. J. *J. Chem. Soc. Dalton Trans.* **2001**, *8*, 1246-1252.

(25) Armstrong, A.; Chivers, T.; Parvez, M.; Boeré, R. *Angew. Chem. Int. Ed.* **2004**, *43*, 502-505.

(26) Drummond, A. M.; Gibson, L. T.; Kennedy, A. R.; Mulvey, R. E.; O'Hara, C. T.; Rowlings, R.B.; Weightman, T. *Angew. Chem. Int. Ed.* **2002**, *41*, 2382-2384.

Table 1. Crystallographic Data

	5a	**9a**•2THF	**11a**	**18**
Formula	$C_{34}H_{74}Al_2N_6P_2Si_2$	$C_{25}H_{59}AlLiN_4O_2PSi$	$C_{34}H_{74}AlLi_2N_4O_4P$	$C_{40}H_{100}Mg_3N_9O_4P_3S_3$
f.w., g	739.07	540.74	674.80	1033.31
space group	$P2_1/c$	$P2_1/c$	$P2_1/c$	P -1
a, Å	20.400(6)	10.209(3)	10.876(2)	14.993(4)
b, Å	16.813(4)	17.616(4)	12.901(3)	15.285(4)
c, Å	12.865(11)	18.975(6)	29.422(7)	15.535(4)
α, deg	90	90	90	96.188(14)
β, deg	92.31(3)	91.218(9)	91.541(13)	102.701(16)
γ, deg	90	90	90	117.474(14)
V, Å^3	4409(4)	3411.7(17)	4126.7(16)	2989.9(14)
Z	4	4	4	2
T, K	173(2)	173(2)	100(2)	173(2)
λ, Å	0.71073	0.71073	0.71073	0.71073
d_{calcd}, g cm^{-3}	1.113	1.053	1.086	1.148
μ, mm^{-1}	0.223	0.17	0.125	0.278
F(000)	1616	1192	1488	1128
R^a	0.044,	0.081	0.23	0.042
$R_w{}^b$	0.107	0.203	0.55	0.096

[a] $R = [\Sigma||F_o| - |F_c||]/[\Sigma |F_o|]$ for reflections with $I > 2.00\sigma(I)$

[b] $R_w = \{[\Sigma w(F_o^2 - F_c^2)^2]/[\Sigma w(F_o^2)^2]\}^{1/2}$ for all reflections

Table 2. Selected Bond Lengths (Å) and Angles (º) for **5a**

P(1)-N(1)	1.5903(15)	P(1)-N(2)	1.5952(15)
P(1)-N(3)	1.6816(16)	Al(1)-C(4)	1.959(2)
Al(1)-C(5)	1.963(2)	Al(1)-N(1)	1.9597(16)
Al(1)-N(2)	1.9251(16)	P(1)-N(3)-P(1)*	96.55(9)
N(3)-P(1)-N(3)*	83.45(9)	N(1)-Al(1)-N(2)	76.40(6)
P(1)-N(1)-Al(1)	92.27(7)	P(1)-N(2)-Al(1)	93.41(7)

Symmetry transformations used to generate equivalent atoms:
#1 -x,-y,-z #2 -x+1,-y,-z+1

Table 3. Selected Bond Lengths (Å) and Angles (º) for **9**

Atoms	X-ray Data for **9a**•2THF	Calcd for **9b**•2OMe_2	Atoms	X-ray Data for **9a**•2THF	Calcd for **9b**•2OMe_2
P(1)-N(1)	1.640(4)	1.642	P(1)-N(2)	1.640(4)	1.643
P(1)-N(3)	1.588(3)	1.611	P(1)-N(4)	1.716(3)	1.755
Al(1)-N(1)	1.911(5)	1.966	Al(1)-N(2)	1.886(4)	1.922
Li(1)-N(3)	1.969(7)	1.933	Li(1)-N(4)	2.178(7)	2.137
Al(1)-C(1)	1.980(5)	1.983	Al(1)-C(2)	1.989(5)	1.986
Li(1)-O(1)	1.993(8)	1.974	N(1)-Al(1)-N(2)	77.85(16)	76.8
N(3)-Li(1)-N(4)	71.6(2)	75.8	P(1)-N(4)-Li(1)	88.9(2)	86.0
P(1)-N(3)-Li(1)	100.6(3)	97.0	P(1)-N(1)-Al(1)	93.9(2)	93.4
P(1)-N(2)-Al(1)	94.9(2)	95.3	N(1)-P(1)-N(2)	93.3(2)	94.5
N(1)-P(1)-N(3)	121.63(19)	123.2	N(3)-P(1)-N(4)	94.71(16)	96.1

Table 4. Selected Bond Lengths (Å) and Angles (º) for **11**

Atoms	X-ray Data for **11a**	Calcd for **11b**	Atoms	X-ray Data for **11a**	Calcd for **11b**
P(1)-N(1)	1.668(9)	1.661	Li(1)-O(1)	2.03(2)	1.960
P(1)-N(2)	1.671(9)	1.661	Li(1)-O(2)	2.15(2)	2.126
P(1)-N(3)	1.645(9)	1.668	Li(2)-O(2)	2.09(2)	2.126
P(1)-N(4)	1.597(10	1.668	Li(2)-O(3)	2.00(2)	1.960
Al(1)-N(1)	1.881(10)	1.918	N(1)-Al(1)-N(2)	77.4(4)	76.7
Al(1)-N(2)	1.877(10)	1.918	N(3)-P(1)-N(4)	91.7(5)	93.2
Li(1)-N(3)	2.07(2)	2.009	N(1)-P(1)-N(2)	89.4(5)	91.5
Li(2)-N(3)	2.01(2)	2.009	Li(1)-N(3)-P(1)	91.0(7)	86.4
Li(1)-N(4)	2.13(2)	2.009	Li(2)-N(4)-P(1)	91.1(7)	86.4
Li(2)-N(4)	1.98(2)	2.009	Li(1)-O(2)-Li(2)	67.1(8)	66.4

Table 5. Experimental and Calculated Hyperfine Coupling Constants (G) for **13** and **14**

Nucleus	Spin	**13a** [a]	**13b** [b]	**14a** [a]	**14b** [b]
^{27}Al	5/2	1.39	-1.22	1.99	-2.03
^{7}Li	3/2	1.43	-1.67	1.40	-1.58
^{31}P	1/2	29.29	-30.72	28.45	-30.96
^{14}N^{t}Bu…Li	1	7.20	6.61	6.44	5.76
^{14}N^{t}Bu…Al	1	1.61	-1.29	1.67	0.50
^{14}N SiMe$_3$	1	0.27	-0.07	-	-

[a] Values used to simulate experimental spectrum.
[b] Values calculated for model systems.

Table 6. Selected Bond Lengths (Å) and Angles (º) for **18**

P(1)-N(1)	1.6078(16)	P(1)-N(2)	1.6532(17)
P(1)-N(3)	1.6721(18)	P(1)-S(1)	2.0112(8)
Mg(1)-O(1)	2.0266(15)	Mg(1)-O(2)	2.1191(15)
Mg(1)-O(3)	2.0030(16)	Mg(2)-O(1)	2.1198(15)
Mg(2)-O(2)	2.0042(15)	Mg(2)-O(3)	2.0325(15)
Mg(3)-O(1)	2.0039(15)	Mg(3)-O(2)	2.0346(16)
Mg(3)-O(3)	2.1208(15)	Mg(1)-N(1)	2.0675(17)
Mg(1)-S(1)	2.6290(10)	Mg(2)-N(4)	2.0686(18)
Mg(2)-S(2)	2.6166(11)	Mg(3)-N(7)	2.0677(18)
Mg(3)-S(3)	2.6237(11)	Mg(1)-Mg(2)	3.0317(12)
N(2)-P(1)-N(3)	100.60(9)	P(1)-S(1)-Mg(1)	75.56(3)
P(1)-N(1)-Mg(1)	102.69(8)	S(1)-Mg(1)-N(1)	74.47(5)
O(1)-Mg(1)-O(2)	83.08(6)	Mg(1)-O(1)-Mg(2)	93.94(6)
S(1)-P(1)-N(1)	104.74(6)	O(1)-Mg(3)-O(2*)	103.21(6)
O(2)-Mg(2)-O(3)	102.40(6)	O(1)-Mg(2)-O(2)	83.60(6)

Symmetry transformations used to generate equivalent atoms:
#1 -x,-y+1,-z

Table 7. Reactivities of $EP(NHR)_3$ towards metal alkyl reagents MR_x

(E, R)	^{n}BuLi	$ZnMe_2$	$AlMe_3$	$MgBu_2$
O, ^{t}Bu	One- or two-fold deprotonation [a]	Three-fold deprotonation; multiple products formed [d]	One- or two-fold deprotonation [e]	Possibly three-fold deprotonation; multiple products formed [f]
S, ^{t}Bu	One- or two-fold deprotonation; sulfur extrusion and dimerization to a metaphosphate [b]	Mono-deprotonation [d]	One- or two-fold deprotonation [f]	Mono-deprotonation; sulfur extrusion at high temperatures [f]
$NSiMe_3$, Cy	Three-fold deprotonation [c]	Mono-deprotonation [d]	Dimerization to metaphosphate [f]	Mono-deprotonation; *NCy*, *$NSiMe_3$* chelation [f]
$NSiMe_3$, ^{t}Bu	Three-fold deprotonation [c]	Mono-deprotonation; *N^tBu*, *$NSiMe_3$* chelation [d]	Mono-deprotonation; *N^tBu*, *$NSiMe_3$* chelation [f]	Mono-deprotonation; *N^tBu*, *NH^tBu* chelation [f]

[a] References 6 and 8
[b] References 8 and 10
[c] Reference 6
[d] Reference 7
[e] Reference 12
[f] This work

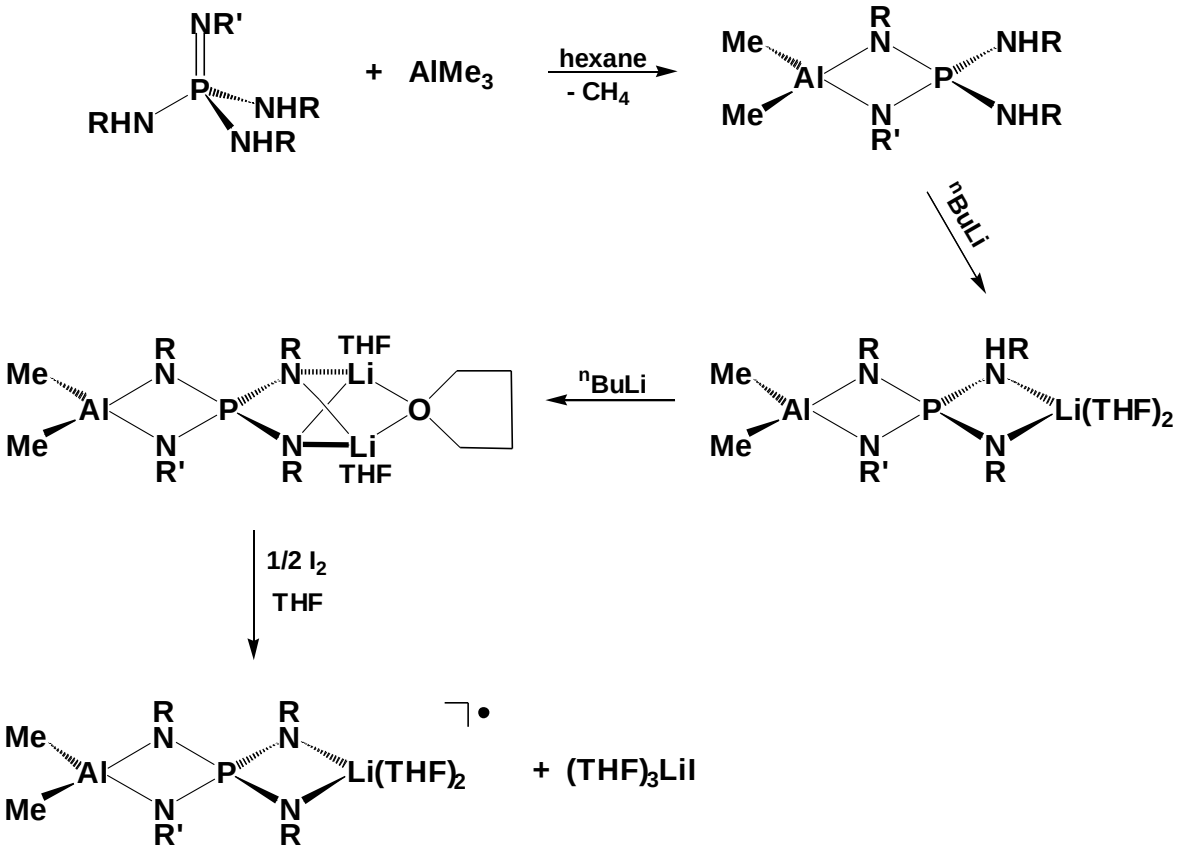

Scheme 1. Step-wise deprotonation of trisamino(imino)phosphates to mixed Me_2Al^+/Li^+ tetraimidophosphate complexes and subsequent oxidation to yield persistent spirocyclic radicals (R = ^{t}Bu; R′ = $SiMe_3$, ^{t}Bu).

Captions for Figures

Figure 1. Thermal ellipsoid diagram of **5a** (30 % probability ellipsoids). Hydrogen atoms omitted for clarity.

Figure 2. Thermal ellipsoid diagram of **9a•**2THF (30 % probability ellipsoids). Only α-carbon atoms of the ^{t}Bu and $SiMe_3$ groups are shown; only oxygen atoms of THF molecules are shown.

Figure 3. Experimental (top) and simulated (bottom) EPR spectra of **13a** in THF.

Figure 4. SOMO of **13b** (left) and **14b** (right)

Figure 5. Experimental (top) and simulated (bottom) EPR spectra of **14a** in THF.

Figure 6. Thermal ellipsoid diagram of **18** (30 % probability ellipsoids). Only α-carbons of *tert*-butyl groups are shown.

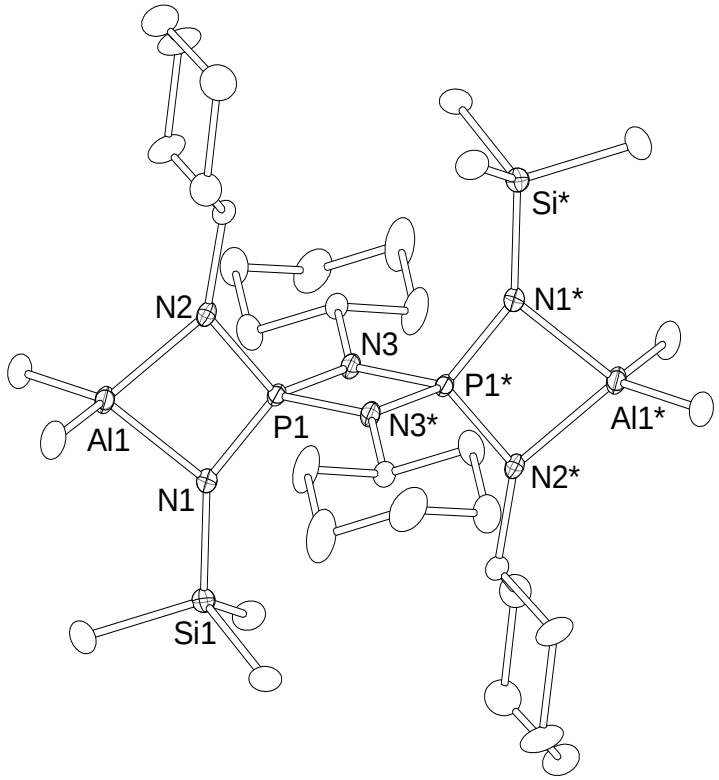

Fig. 1

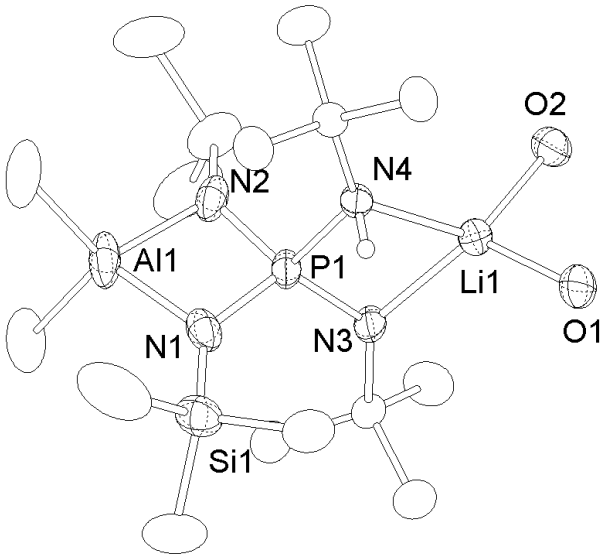

Fig. 2

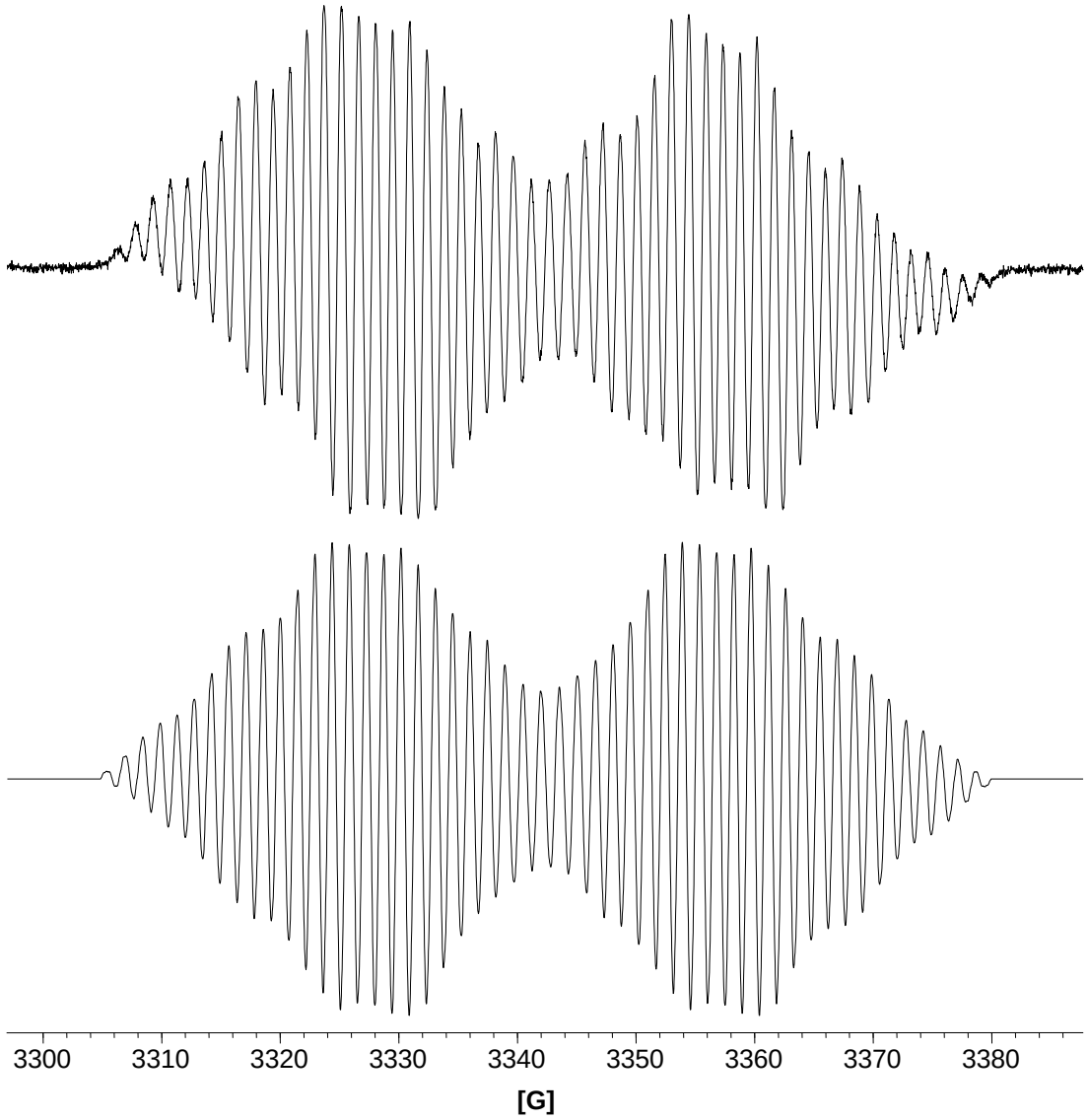

Fig. 3

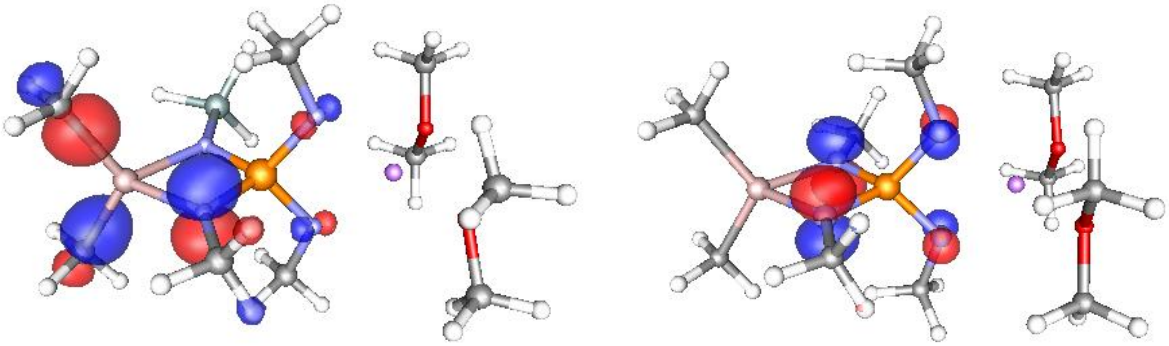

Fig. 4

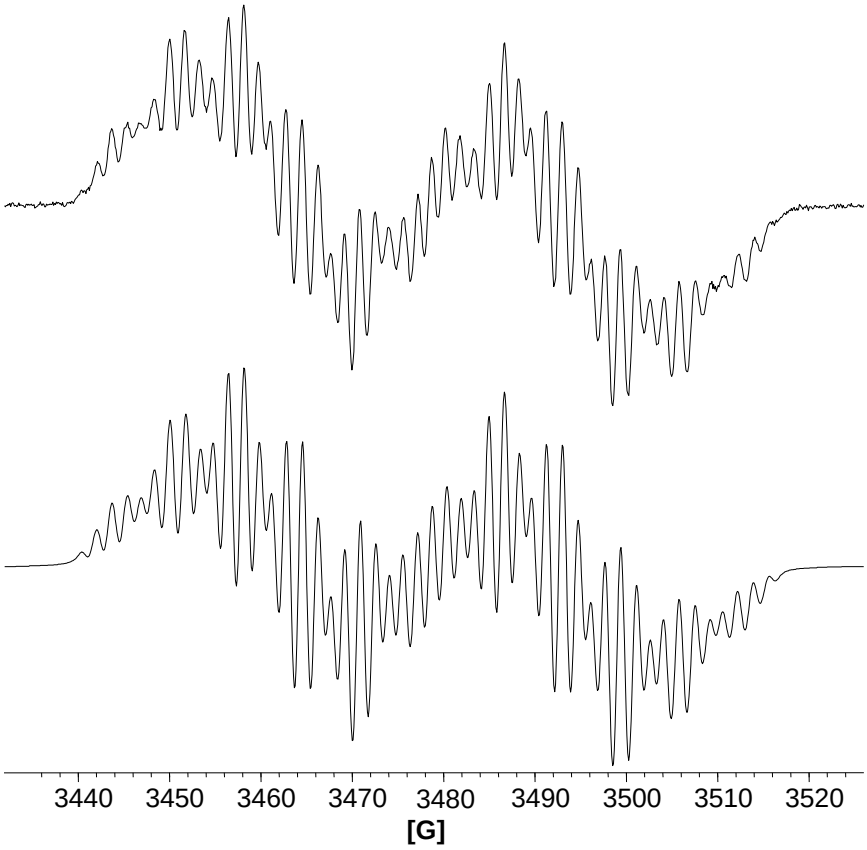

Fig. 5

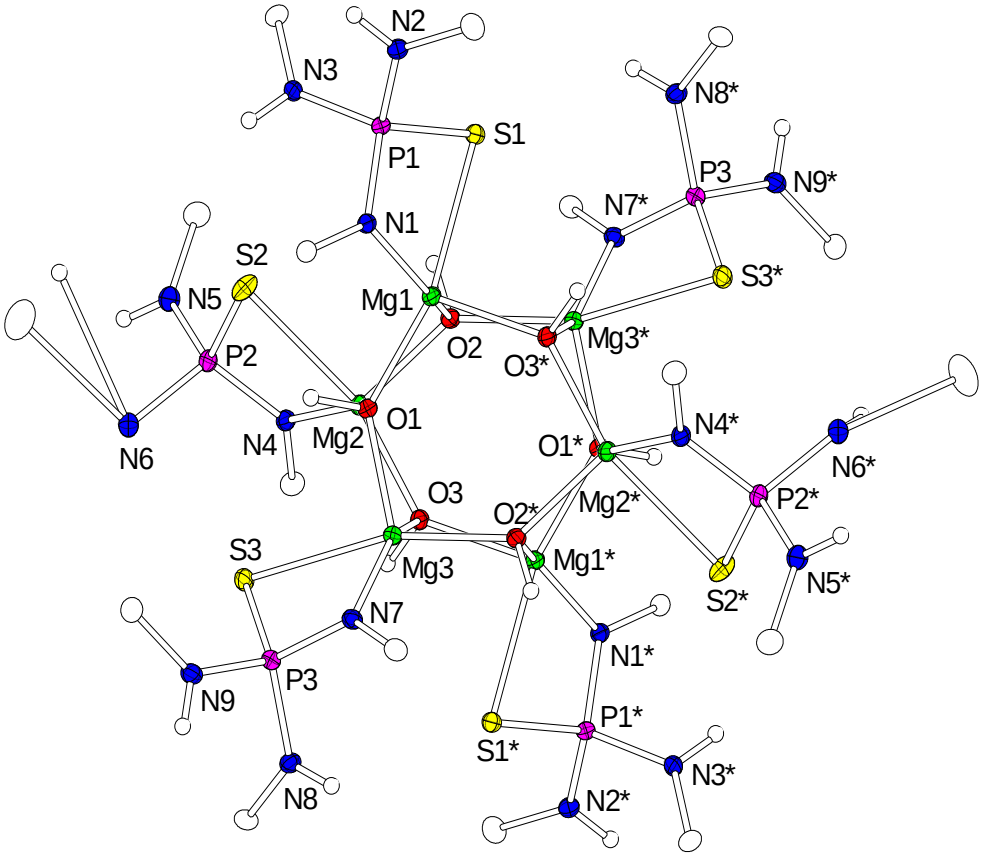
N2
N3
S1
P1
N1
N8*
P3
N9*
N7*
S3*
S2
N5
Mg1
O2
Mg3*
O3*
P2
O1
N6
N4
Mg2
O1*
N4*
N6*
O3
O2*
Mg2*
P2*
S3
Mg3
Mg1*
S2*
N5*
N7
N1*
P3
N9
P1*
S1*
N3*
N8
N2*

Fig. 6